Journal of Inorganic and Organometallic Polymers and Materials (2020) 30:169–173
https://doi.org/10.1007/s10904-019-01390-y

Electrochemical Measurement of Bismuth Clusters in Dendrimer Through Transformation from Atomicity Controlled Complexes

Tetsuya Kambe[1,2] · Shotaro Imaoka[1] · Risaki Hasegawa[1] · Takamasa Tsukamoto[1,2] · Takane Imaoka[1,2] · Keisuke Natsui[3] · Yasuaki Einaga[3] · Kimihisa Yamamoto[1,2]

Received: 24 June 2019 / Accepted: 15 November 2019 / Published online: 21 November 2019

Abstract
Dendrimers can provide unique reaction space for sub-nano sized materials. Recently, we have demonstrated a luminous bismuth dendrimer and the on/off switching by stepwisely assembled bismuth units in a phenylazomethine dendrimers. In addition, formation of bismuth clusters was also demonstrated by the reduction of the bismuth salts assembled in the dendrimer. In this study, we have revealed the atomicity dependency about the reduction and oxidation potentials of the assembled bismuth complexes and clusters, respectively. The measurements were conducted by the electrochemical process of the bismuth assembled dendritic poly-phenylazomethines.

Keywords Dendrimers · Bismuth · Sub-nano sized clusters

1 Introduction

Sub-nano sized metal clusters are fascinating materials that can provide remarkable properties. For example, extraordinary high catalytic activities were demonstrated by platinum or other clusters [1–6]. In spite of such attracting properties, the synthesis is still difficult because the ways to control the atomicity of the clusters were limited. In addition, the clusters with several atoms have the unique properties that can not be shown in the clusters with other atomicity even though they have similar sizes. The feature is clearly reflected in magic numbered Au clusters [7, 8] and high catalytic activity of the Pt_{12} cluster [9, 10]. Therefore, control of the atomicity in a cluster is necessary to reveal the properties.

Polymer-protection is a useful tool to handle such clusters since it can enhance stability of the inner clusters. Coordinating polymer ligands with sulfur or phosphine ligands can provide high stabilization effect for various clusters or particles [11–21], and some stable gold or silver clusters were subjected to single-crystal analysis, optical measurement and other measurements. However, these strong protections often change the electronic state of the clusters. On the other hand, protections by polymer capsules are soft compared to those by coordinating ligands. They are often used as a catalyst by tuning the conformation of polymers [22–24]. Uniformly branched polymers called "Dendrimers" [25–28] can also protect such clusters in the inner cavity. The soft protection by the branches of the dendrimers is utilized for highly active catalysts with inherent properties of the metal clusters [29–32].

Here, we used phenylazomethine dendrimers called DPAs (Fig. 1) [33–36]. The DPAs have not only an inner cavity which can protect the sub-nano sized clusters, but also designed π-conjugated branches that can control the number of assembled metals. The number is controlled by the imine parts on the branches of the DPAs which can coordinate to metal salts. The gradually changed basicity of the imines provided stepwise metal assembly. Due to the stepwise assembly of the metals, precisely controlled

Electronic supplementary material The online version of this article (https://doi.org/10.1007/s10904-019-01390-y) contains supplementary material, which is available to authorized users.

✉ Kimihisa Yamamoto
yamamoto@res.titech.ac.jp

[1] Laboratory for Chemistry and Life Science, Tokyo Institute of Technology, Yokohama 226-8503, Japan

[2] JST-ERATO, Tokyo Institute of Technology, Yokohama 226-8503, Japan

[3] Department of Chemistry, Keio University, 3-14-1 Hiyoshi, Yokohama 223-8522, Japan

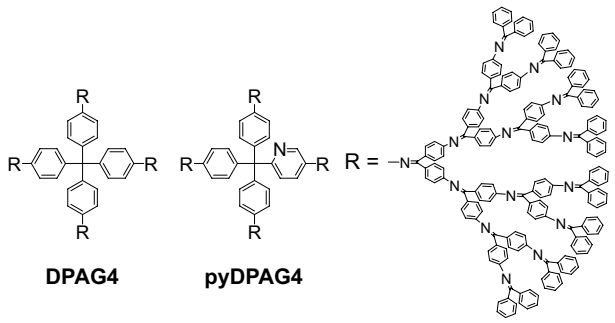

Fig. 1 Chemical structures of DPAG4 ($C_{805}H_{560}N_{60}$) and pyDPAG4 ($C_{804}H_{559}N_{61}$)

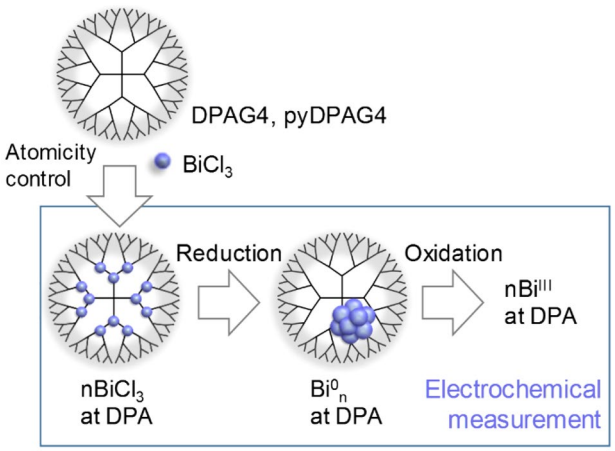

Fig. 2 Schematic illustration of electrochemical reactions about atomicity controlled clusters in the dendrimers

metal clusters at atomicity level can be prepared in the DPAs [9, 37–45].

Our recent progress promoted preparation of functional bismuth in the DPAs [46–49]. We investigated tunable photo-luminescence, solid-state emission and optical switching of the bismuth assembled DPAs. In addition, synthesis of bismuth clusters in the DPAs was succeeded by using polyvinylpyrrolidone. Through these studies, the electrochemical synthesis of the bismuth clusters in the DPAs was suggested [46]. In this study, we have revealed the atomicity dependency of the transformation between the bismuth complexes and the corresponding clusters by using the DPA templates (Fig. 2). The control of the atomicity was achieved through the finely controlled metal assembly process of the $BiCl_3$ into the DPA in the solution with sufficient electrolytes. Through the observation of reduction and oxidation phenomena of the assembled bismuth, the dependency on the atomicity was clarified.

2 Experimental Sections

2.1 Materials

$BiCl_3$ ultra dry and Bu_4NPF_6 were purchased from Alfa Aesar and Sigma-Aldrich. Dehydrated acetonitrile and chloroform were obtained from Kanto Chemicals and Wako Pure Chemical Industries, Ltd., respectively. The DPAG4 and pyDPAG4 was synthesized according to the literatures [36, 50]. The boron-doped diamond electrode was prepared according to the previous reports [51, 52].

2.2 Characterization

UV–Vis absorption spectra were measured using Shimazu UV-3100PC spectrometer with a quartz cell having an optical length of 1 cm. Cyclic voltammetry was conducted by using BAS ALS750B analyzer. Scanning transmission electron microscopy (STEM) images were obtained using JEM-ARM200F (JEOL) or JEM-2100F (JEOL) with samples deposited on a Cu mesh microgrid (Okenshoji Co.)

2.3 UV–Vis Titration of $BiCl_3$ Added to the DPAG4 Solution with Bu_4NPF_6

Acetonitrile solution of $BiCl_3$ (6.29 mM) and acetonitrile/chloroform (1/1) solution of the DPAG4 (2.67 μM) were prepared in an Ar-filled glove box. Then the aimed equivalent of $BiCl_3$ solution was added to the DPAG4 solution (3.0 mL) at the quartz cell. Then the solution was shaken to promote complexation. The complexation process to the DPAG4 was monitored by UV–Vis absorption spectra from 0 to 60 equivalents. The stepwise assembly was judged by the isosbestic points observed around 370 nm.

2.4 Cyclic Voltammetry of the Bismuth Complexes in the DPAs

Preparation and measurements were totally conducted in an Ar-filled glove box. An acetonitrile solution of $BiCl_3$ (3–6 mM) was added to an acetonitrile/chloroform (1/1) mixed solution of the DPAG4 or pyDPAG4 with Bu_4NPF_6 (0.1 M). The concentrations of the DPAG4 were 3 μM for DPAG4-8$BiCl_3$ and DPAG4-12$BiCl_3$, 1 μM for DPAG4-28$BiCl_3$ and 0.5 μM for DPAG4-60$BiCl_3$. That of pyDPAG4 was 3 μM. The added amount of the $BiCl_3$ solution was determined according to the aimed equivalents to the DPAG4. The mixed solution was vigorously stirred for the complexation. A glassy carbon disc electrode and a rolled platinum wire were used as the working and counter electrodes, respectively. An Ag^+/Ag (0.01 M $AgNO_3$ in 0.1 M

Bu_4NClO_4/acetonitrile) electrode was used as a reference electrode. The equipped electrodes were connected to the potentiostat through a flange with conduction path for measurements.

3 Results and Discussions

The transformation between the metal complexes and the clusters in the dendrimer was conducted after preparation of the bismuth assembled metallodendrimers. They were prepared in an acetonitrile/chloroform solution with Bu_4NPF_6 (0.1 M) as an electrolyte. The number of the bismuth atom in one cluster was determined in the complexation process of the $BiCl_3$ to the DPAG4. The controlled assembly of $BiCl_3$ was confirmed by a UV–Vis titration. The spectral change and the titration curve are shown in Fig. 3. The titration curve was slightly changed compared with that without electrolytes. However, the stepwise shift in the isosbestic point maintains in the electrolyte case. The equivalents of the added $BiCl_3$ showing each isosbestic point were consistent with the numbers of imines at each layer of the DPAG4. It confirmed atomicity controlled assembly of the bismuth units in the dendrimer. The DPAG4 was used for the assembly of 12, 28 and 60 $BiCl_3$. 13 $BiCl_3$ was carried out with the dendrimer equipped with one pyridine part (pyDPAG4). In addition, a 8 $BiCl_3$ assembled sample was prepared with the DPAG4. Though the number of 8 is different from the number of imines in the DPAG4, the atomicity can be controlled under 12 atoms by the potential gradient in the DPAG4 [9].

The coordinated bismuth units in the DPAs were subjected to the electrochemical measurement with a potentiostat. The reduction peaks around −0.5 V versus Ag/Ag^+ in a potential cycling measurement showed reaction from Bi^{III} to Bi^0. The bismuth salts changed to clusters in the DPAG4 by the chronoamperometric reduction, which was demonstrated by STEM observation for a sample prepared by applying negative voltage to the bismuth-assembled dendrimers on the carbons [46]. The observed cluster size (1.5 ± 0.3 nm) was clearly smaller than that of bismuth-assembled dendrimers (2.2 ± 0.4 nm, Fig. S1). Then, the oxidation potentials of the reduced cluster samples were measured by the linear oxidation sweep after the reduction process. The oxidation peaks were observed from −0.3 to 0 V versus Ag/Ag^+ (Fig. 4). The intensity of the peaks supported oxidation to Bi^{III} by this process.

The initial reduction peaks were derived from the coordinated $BiCl_3$ on the branches. It was well confirmed by the linear increasing of the reduction current according to the equivalent of the assembled $BiCl_3$ (Fig. 5). These results supported successful preparation of the aimed bismuth clusters in the DPAG4.

The oxidation process can be influenced by the property of the synthesized bismuth cluster. The oxidation waves of the clusters showed a simplified form (Fig. 4). It was different from a bulk bismuth metal showing several peaks [46]. Such several peaks were observed by increasing concentration of the DPAG4-28$BiCl_3$ sample (Fig. S2), indicating generation of aggregated forms by the reduction process. By contrast, such aggregation peaks

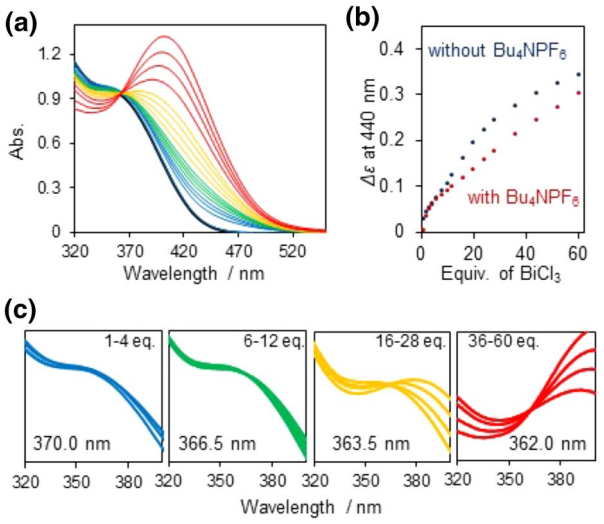

Fig. 3 **a** UV–Vis titration spectra demonstrating stepwise assembly of $BiCl_3$ into the DPAG4 in the solution with Bu_4NPF_6. **b** Titration curves about the addition of $BiCl_3$ with and without electrolyte. **c** Four isosbestic points observed during the titration. Each isosbestic point corresponds to the layer of the DPAG4 template

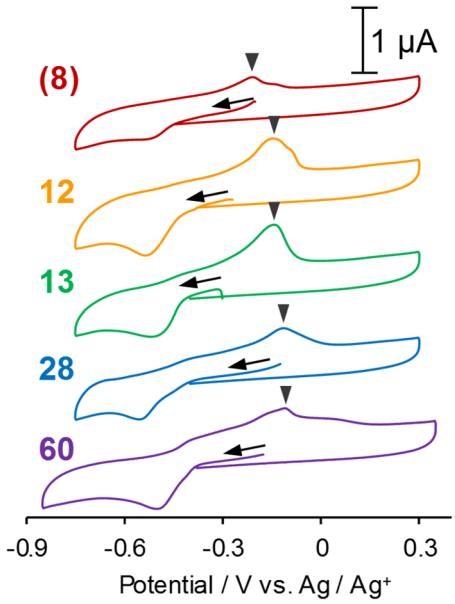

Fig. 4 Electrochemical voltammetry of the bismuth assembled DPAG4

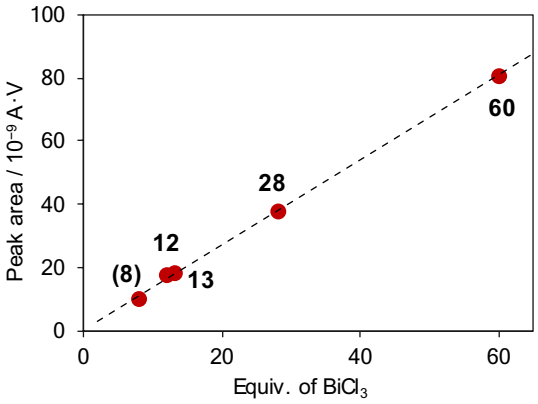

Fig. 5 Relation between the reduction peak areas and equivalents of the assembled $BiCl_3$ in the DPAs. A dotted line is linear fitting of the data

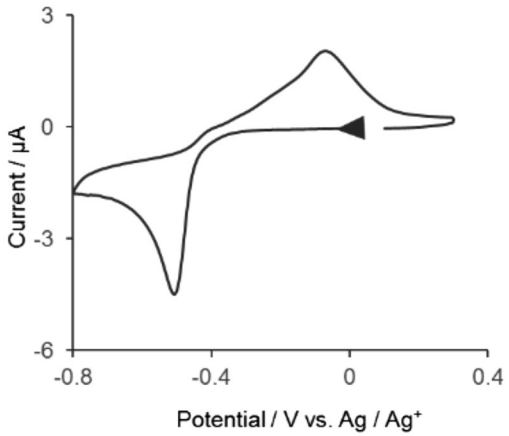

Fig. 6 Cyclic voltammograms of 28$BiCl_3$-TPMG4 (3 µM) at 10 mV/s with the boron-doped diamond electrode

were not detected in the low concentration. Therefore, the observed oxidation potentials suggested properties of the clusters. The oxidation peaks shifted to the negative value as the atomicity decreased (black triangles in Fig. 4). It suggested destabilization of the small clusters.

Electrochemical measurement using 1% boron-doped diamond electrodes [51, 52] was found to be effective to control the aggregation of bismuth at the reduced state. The set-up is shown in Fig. S3. The observed cyclic voltammogram of the DPAG4-28$BiCl_3$ sample at 3 µM demonstrated a simple oxidation peak (Fig. 6), and it was clearly different from that in the aggregation case observed by using glassy carbon disc electrode as shown in the Fig. S2. This improvement is considered to be derived from high chemical stability available at the surface of the boron-doped diamond electrode [51–61].

4 Conclusion

We revealed the transformation process of the metal complex and the clusters by the electrochemical reduction and oxidation in the DPAG4. The atomicity dependency was observed in the oxidation process, and it was not observed in the initial reduction of the bismuth complexes. The negative shift of the oxidation potential suggested destabilization of the clusters.

Acknowledgements This study was supported by JSPS KAKENHI Grant Numbers 17K05804 and 15H05757, the ERATO program of the Japan Science and Technology (JST) Agency (JPMJER1503), and the cooperative research program of the Network Joint Research Center for Materials and Devices of Japan.

Author Contributions The manuscript was written through the contributions of all authors. All authors have given approval to the final version of the manuscript.

Compliance with Ethical Standards

Conflict of interest The authors declare no competing financial interest.

References

1. S. Vajda, M.J. Pellin, J.P. Greeley, C.L. Marshall, L.A. Curtiss, G.A. Ballentine, J.W. Elam, S. Catillon-Mucherie, P.C. Redfern, F. Mehmood, P. Zapol, Nat. Mater. **8**, 213–216 (2009)
2. Y. Lei, F. Mehmood, S. Lee, J. Greeley, B. Lee, S. Seifert, R.E. Winans, J.W. Elam, R.J. Meyer, P.C. Redfern, D. Teschner, R. Schlögl, M.J. Pellin, L.A. Curtiss, S. Vajda, Science **328**, 224–228 (2010)
3. E. Fernández, M.A. Rivero-Crespo, I. Domínguez, P. Rubio-Marqués, J. Oliver-Meseguer, L. Liu, M. Cabrero-Antonino, R. Gavara, J.C. Hernández-Garrido, M. Boronat, A. Leyva-Pérez, A. Corma, J. Am. Chem. Soc. **141**, 1928–1940 (2019)
4. T. Imaoka, Y. Akanuma, N. Haruta, S. Tsuchiya, K. Ishihara, T. Okayasu, W.-J. Chun, M. Takahashi, K. Yamamoto, Nat. Commun. **8**, 688 (2017)
5. T. Imaoka, K. Yamamoto, Bull. Chem. Soc. Jpn **92**, 941–948 (2019)
6. E.C. Tyo, S. Vajda, Nat. Nanotechnol. **10**, 577–588 (2015)
7. H.-G. Boyen, G. Kaestle, F. Weigl, B. Koslowski, C. Dietrich, P. Ziemann, J.P. Spatz, S. Riethmueller, C. Hartmann, M. Moeller, G. Schmid, M.G. Garnier, P. Oelhafen, Science **297**, 1533–1536 (2002)
8. Y. Negishi, Y. Takasugi, S. Sato, H. Yao, K. Kimura, T. Tsukuda, J. Am. Chem. Soc. **126**, 6518–6519 (2004)
9. T. Imaoka, H. Kitazawa, W.-J. Chun, K. Yamamoto, Angew. Chem. Int. Ed. **54**, 9810–9815 (2015)
10. T. Imaoka, K. Yamamoto, J. Surf. Sci. Soc. Jpn. **38**, 2017/12/17 (2017)
11. A. S. Abd-El-Aziz, C. E. Carraher, C. U. Pittman, M. Zeldin, Macromolecules containing metal and metal-like elements, Volume 7: Nanoscale interactions of metal-containing polymers. ISBN: 978-0-471-77325-2 (2005)

12. Y. Negishi, K. Nobusada, T. Tsukuda, J. Am. Chem. Soc. **127**, 5261–5270 (2005)
13. S. Yamazoe, K. Koyasu, T. Tsukuda, Acc. Chem. Res. **47**, 816–824 (2014)
14. C. Sanchez, G.J.A.A. de Soler-Illia, F. Ribot, T. Lalot, C.R. Mayer, V. Cabuil, Chem. Mater. **13**, 3061–3083 (2001)
15. M.T. Reetz, G. Lohmer, Chem. Commun. **16**, 1921–1922 (1996)
16. M. Zhu, C.M. Aikens, F.J. Hollander, G.C. Schatz, R. Jin, J. Am. Chem. Soc. **130**, 5883–5885 (2008)
17. G. Schmid, R. Pfeil, R. Boese, F. Brandermann, S. Meyer, G.H.M. Calis, J.W.A. Van der Velden, Chem. Ber. **114**, 3634–3642 (1981)
18. Y. Shichibu, Y. Negishi, T. Tsukuda, T. Teranishi, J. Am. Chem. Soc. **127**, 13464–13465 (2005)
19. O. Lopez-Acevedo, K.A. Kacprzak, J. Akola, H. Hakkinen, Nat. Chem. **2**, 329–334 (2010)
20. M. Knorr, F. Guyon, A. Khatyr, C. Daschlein, C. Strohmann, S. M. Aly, A. S. Abd-El-Aziz, D. Fortinc, P. D. Harvey, Dalton Trans. 948–955 (2009)
21. M.H. Freeman, J.R. Hall, M.C. Leopold, Anal. Chem. **85**, 4057–4065 (2013)
22. J. Kobayashi, Y. Mori, K. Okamoto, R. Akiyama, M. Ueno, T. Kitamura, S. Kobayashi, Science **304**, 1305–1308 (2004)
23. R. Akiyama, S. Kobayashi, J. Am. Chem. Soc. **125**, 3412–3413 (2003)
24. Y. Uozumi, R. Nakao, Angew. Chem. Int. Ed. **42**, 194–197 (2003)
25. D.A. Tomalia, H. Baker, J. Dewald, M. Hall, G. Kallos, S. Martin, J. Roeck, J. Ryder, P. Smith, Polym. J. **17**, 117 (1985)
26. D.A. Tomalia, S.N. Khanna, Chem. Rev. **116**, 2705 (2016)
27. D. Astruc, F. Chardac, Chem. Rev. **101**, 2991 (2001)
28. G.R. Newkome, Z.Q. Yao, G.R. Baker, V.K. Gupta, J. Org. Chem. **50**, 2003 (1985)
29. D. Astruc, F. Lu, J.R. Aranzaes, Angew. Chem. Int. Ed. **44**, 7852–7872 (2005)
30. R.M. Crooks, M. Zhao, L. Sun, V. Chechik, L.K. Yeung, Acc. Chem. Res. **34**, 181–190 (2001)
31. L. Balogh, D.A. Tomalia, J. Am. Chem. Soc. **120**, 7355–7356 (1998)
32. A.W. Bosman, R. Vestberg, A. Heumann, J.M.J. Frechet, C.J. Hawker, J. Am. Chem. Soc. **125**, 715–728 (2003)
33. K. Yamamoto, M. Higuchi, S. Shiki, M. Tsuruta, H. Chiba, Nature **415**, 509 (2002)
34. K. Yamamoto, T. Imaoka, Acc. Chem. Res. **47**, 1127 (2014)
35. M. Higuchi, S. Shiki, K. Ariga, K. Yamamoto, J. Am. Chem. Soc. **122**, 4414 (2001)
36. O. Enoki, H. Katoh, K. Yamamoto, Org. Lett. **5**, 569 (2006)
37. K. Yamamoto, T. Imaoka, W.-J. Chun, O. Enoki, H. Katoh, M. Takenaga, A. Sonoi, Nat. Chem. **1**, 397 (2009)
38. T. Imaoka, H. Kitazawa, W.-J. Chun, S. Omura, K. Albrecht, K. Yamamoto, J. Am. Chem. Soc. **135**, 13089 (2013)
39. M. Takahashi, T. Imaoka, Y. Hongo, K. Yamamoto, Angew. Chem. Int. Ed. **52**, 7419 (2013)
40. M. Takahashi, H. Koizumi, W.-J. Chun, M. Kori, T. Imaoka, K. Yamamoto, Sci. Adv. **3**, e1700101 (2017)
41. T. Imaoka, M. Fushimi, A. Kimoto, Y. Okamoto, K. Takanashi, K. Yamamoto, Chem. Lett. **43**, 1269 (2014)
42. T. Kambe, N. Haruta, T. Imaoka, K. Yamamoto, Nat. Commun. **8**, 2046 (2017)
43. N. Satoh, T. Nakashima, K. Kamikura, K. Yamamoto, Nat. Nanotechnol. **3**, 106 (2008)
44. Y. Inomata, K. Albrecht, K. Yamamoto, ACS Catal. **8**, 451 (2018)
45. I. Hirano, T. Imaoka, K. Yamamoto, J. Inorg. Organomet. Polym Mater. **23**, 223 (2013)
46. T. Kambe, A. Watanabe, T. Imaoka, K. Yamamoto, Angew. Chem. Int. Ed. **55**, 13151 (2016)
47. T. Kambe, R. Hosono, T. Imaoka, K. Yamamoto, J. Photopolym. Sci. Technol. **31**, 311–314 (2018)
48. T. Kambe, T. Imaoka, K. Yamamoto, J. Inorg. Organomet. Polym. **28**, 463–466 (2018)
49. T. Kambe, S. Imaoka, T. Imaoka, K. Yamamoto, J. Nanopart. Res. **20**, 118 (2018)
50. H. Kitazawa, K. Albrecht, K. Yamamoto, Chem. Lett. **41**, 828–830 (2012)
51. Y. Einaga, Bull. Chem. Soc. Jpn **91**, 1752–1762 (2018)
52. M. Tomisaki, S. Kasahara, K. Natsui, N. Ikemiya, Y. Einaga, J. Am. Chem. Soc. **141**, 7414–7420 (2019)
53. K. Natsui, C. Yamaguchi, Y. Einaga, Phys. Status Solidi A **213**, 2081–2086 (2016)
54. Y. Einaga, J. Appl. Electrochem. **40**, 1807–1816 (2010)
55. T.A. Ivandini, Y. Einaga, Chem. Commun. **53**, 1338–1347 (2017)
56. N. Ikemiya, K. Natsui, K. Nakata, Y. Einaga, ACS Sustain. Chem. Eng. **6**, 8108–8112 (2018)
57. K. Nakata, T. Ozaki, C. Terashima, A. Fujishima, Y. Einaga, Angew. Chem. Int. Ed. **53**, 871–874 (2014)
58. P.K. Jiwanti, K. Natsui, K. Nakata, Y. Einaga, RSC Adv. **6**, 102214–102217 (2016)
59. N. Ikemiya, K. Natsui, K. Nakata, Y. Einaga, RSC Adv. **7**, 22510–22514 (2017)
60. J. Xu, K. Natsui, S. Naoi, K. Nakata, Y. Einaga, Diam. Relat. Mater. **86**, 167–172 (2018)
61. M. Tomisaki, K. Natsui, N. Ikemiya, K. Nakata, Y. Einaga, ChemistrySelect **3**, 10209–10213 (2018)